Nanoscience and Nanotechnology Letters
Vol. 4, 338–343, 2012

One-Step Growth and Shaping by a Dual-Plasma Reactor of Diamond Nanocones Arrays for the Assembling of Stable Cold Cathodes

S. Orlanducci[1], V. Guglielmotti[1], I. Cianchetta[1], V. Sessa[1], E. Tamburri[1], F. Toschi[1], M. L. Terranova[1,*], and M. Rossi[2,*]

[1] *Department of Chemical Science and Technology, University of Rome 'Tor Vergata', 00133, Roma, Italy*
[2] *Department of Fundamental and Applied Sciences for Engineering, Sapienza University, 00161, Roma, Italy*

Arrays of conical-shaped nanodiamond structures are formed on silicon substrate by a single-step CVD process from CH_4/H_2 mixtures. The formation of these nanocones has been found to depend on interplay between growing and etching during the CVD process carried out in a dual-mode MW/RF plasma reactor. Morphology and structure of the conical-like systems can be controlled by varying the process parameters, and have been investigated by scanning electron microscopy (SEM), reflection high energy electron diffraction (RHEED) and micro-Raman spectroscopy. The Field Emission (FE) properties of different diamond nanocones arrays have been investigated and compared with those of analogous systems in order to assess the feasibility of the present nanomaterials as electron emitters for cold cathodes. The FE behavior is discussed taking into account the structure of the different diamond nanocones.

Keywords: Diamond, Nanocones, Cold Cathodes, Electron Diffraction.

1. INTRODUCTION

Diamond nanostructures have an edge over other materials for a variety of applications, ranging from optoelectronics to electron emission technology.[1–4] Nanodiamond systems couple indeed the outstanding characteristics of the diamond phase with the ultimate quantum properties of the material at the nanoscale. However, in the nano-world the properties vary with the size and the morphology of the objects and this peculiarity motivated the increasing interest for designing and realizing nanodiamonds systems with shapes as close as possible to those required by the specific application. Considering the substantial impact that these materials have on technology it is nowadays a challenging task to find ways for fabrication of low-dimensional diamond systems with well-defined geometries.

Diamond nanorods and nanocones have been usually realized applying a reactive ion etching (RIE), maskless or not, on almost all kinds of diamond substrates.[3–8] The obtained elongated nanostructures range from poly- to single-crystalline in nature, and sometimes consist of diamond-graphite heterostructures. Some other methodologies to obtain diamond nanostructures consist on hydrogen plasma treatment on CNTs and on nanodiamond films.[9,10] Some nanosized diamond-graphite heterostructures have been obtained by one-step micro wave (MW) CVD synthesis.[11,12]

In this context, the objective of our research is to assess the feasibility to produce a wide range of nanodiamond structures, differing in the shape of the individual entities or in their mutual organization. In the past, the controlled growth of diamond nanoparticles on carbon nanotube bundles has been reported.[13]

More recently, a series of differently shaped nanodiamond structures have been prepared by surface-assisted self-assembly of detonation nanodiamond[14,15] whereas nanowires/whiskers of diamond have been produced by H-etching of diamond deposits using a dual-mode MW/RF plasma.[16]

We report here our more recent results on the synthesis of diamond nanocones using a Plasma Enhanced–Chemical Vapor Deposition (PE-CVD) technique. In particular a maskless single step process has been optimized to produce a large area coating of diamond nanocones. Field Emission characteristics of different kind of samples have been also examined and discussed in terms of diamond nanocones structure and array density.

*Authors to whom correspondence should be addressed.

 1941-4900/2012/4/338/006 doi:10.1166/nnl.2012.1312

2. EXPERIMENTAL DETAILS

The diamond nanocones were grown using a PE-CVD reactor where a MW generator capacitively coupled to a RF system is used for activation of the gas phase. The working frequencies of the MW and RF generators were 2.46 GHz and 13.56 MHz. respectively, and the MW and RF power supply provided 300 W and 50 W. A detailed description of the MW/RF reactor can be found in Ref. [17].

The flow rates of the CH_4 and H_2 gaseous reactants were varied from 2 sccm to 10 sccm and 100 to 90 sccm, respectively, and the reactor operating pressure was 2 mbar. The deposition temperature was fixed at 700 °C. The substrates used in these experiments were Si plates preliminary polished by sonication using a dispersion of diamond powder (0.25 μm). The reported results have been obtained from samples, namely A1 and A2, obtained with the lowest and highest *C* concentrations, respectively.

The morphology of the deposit was examined by FE-SEM and the structural characterization of the cones was carried out using micro-Raman and RHEED.

The micro-Raman spectra were acquired using aAr ion laser (514.5 nm, 1 mW power) and a 600 gr/mm grating spectrometer (iHR550 Horiba JobinYvon) coupled with a liquid-nitrogen cooled CCD.

Reflection high energy electron diffraction (RHEED) observations have been performed at 60 keV on an electron optics column AEI EM6G, equipped with a high resolution diffraction stage.

The field emission characteristics were investigated using a custom-designed FE apparatus. Along with the *I*/*V* curves other important data, such as emission threshold, current density and current stability were registered and analysed. The FE current was measured at room temperature and at a working pressure of 10^{-7} mbar using as anode a Mo sphere with a diameter of 1.00 ± 0.05 mm. The samples have been tested at a fixed anode-cathode distance, determined by a capacitive approach using a LRC meter. For each deposit more than 20 different areas have been tested.

3. RESULTS AND DISCUSSION

The deposition runs produced arrays of conical-shaped objects protruding from the substrate surface. Differences in cone shapes and array densities seem to be originated from different concentrations of the *C* source. The FE-SEM imagesof two typical deposits obtained by 30 min lasting PE-CVD processes using 2 sccm (sample A1) and 10 sccm (sample A2) of CH_4 are reported in Figures 1(a)–(b) and (c)–(d), respectively. Sample A1 (Figs. 1(a–b)) exhibits a lower density of cones with a regular shape, whereas sample A2 is composed by a dense assemble of irregularly shaped conical objects (Figs. 1(c–d)).

Larger magnification plain-view FE-SEM images reported in Figures 2(a)–(b) evidence the shape and detail the tips of some representative isolated structures grown on sample A1 and A2, respectively. The protruding structures of sample A1 are rather uniform in size and apical angle, whereas those of sample A2 are more irregular in size and show ahelicoidal cone shape, that can appear in the top view micrograph (Fig. 2(b)) an overlapping of cylinder with decreasing diameters.

Information on the structure of such elongated deposits has been obtained by a RHEED analysis carried out at

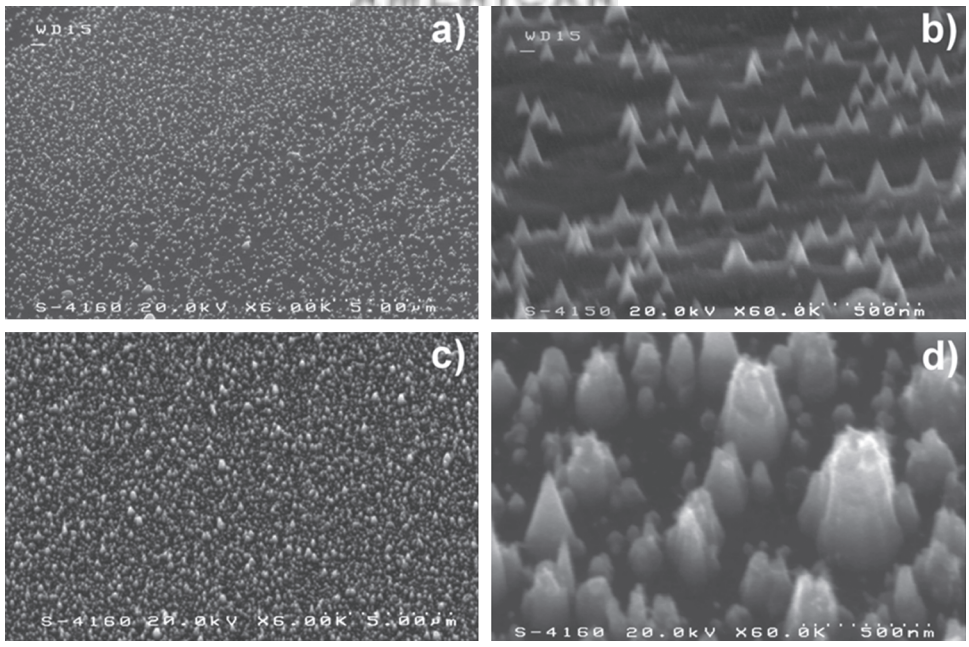

Fig. 1. FE-SEM images of deposits obtained by 30 min lasting PE-CVD processes using: (a) and (b) 2 sccm of CH_4; (c) and (d) 10 sccm of CH_4.

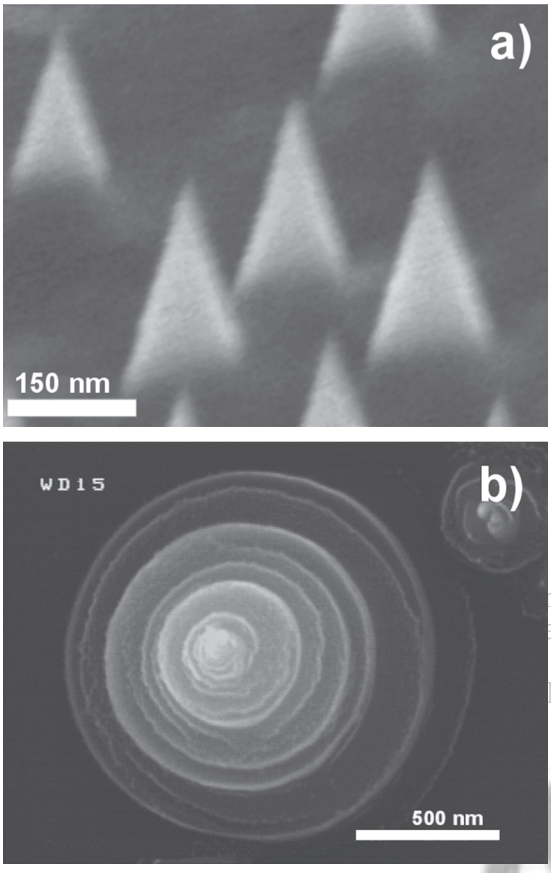

Fig. 2. Images in the foreground of the different conical shapes characterizing sample A1 (a) and sample A2 (b).

a very glancing angle of incidence with respect to the substrate, thus obtaining diffraction signals in transmission conditions. The ED patterns and the reference data reported in Figure 3 enabled us to identify the presence of the diamond phase (Fd3m s.g.) in both samples. The broadening of the rings in the radial direction can be ascribed to the nanometric sizes of the diamond crystallites. Some fine details of ED patterns deserve some further comments.

In particular, the pattern of sample A1 (Fig. 3(a)) evidences also the presence of additional weak Debye's rings (white arrows) that can be attributed to a strongly minority presence of graphite. Instead, the pattern of sample A2 (Fig. 3(b)) does not reveal the presence of a second crystalline phase (all the Debye's rings have to be attributed to the diamond phase) but it is characterized by a relatively strong hazy background that can be explained taking into account the presence of amorphous material, practically absent in sample A1.

A complementary insight into the structural and chemical features of the samples was achieved by Raman spectroscopy.

Raman spectra of sample A1 and A2 are reported in Figures 4(a) and (b), respectively. For both samples is evident the presence of a broadened peak centred at about

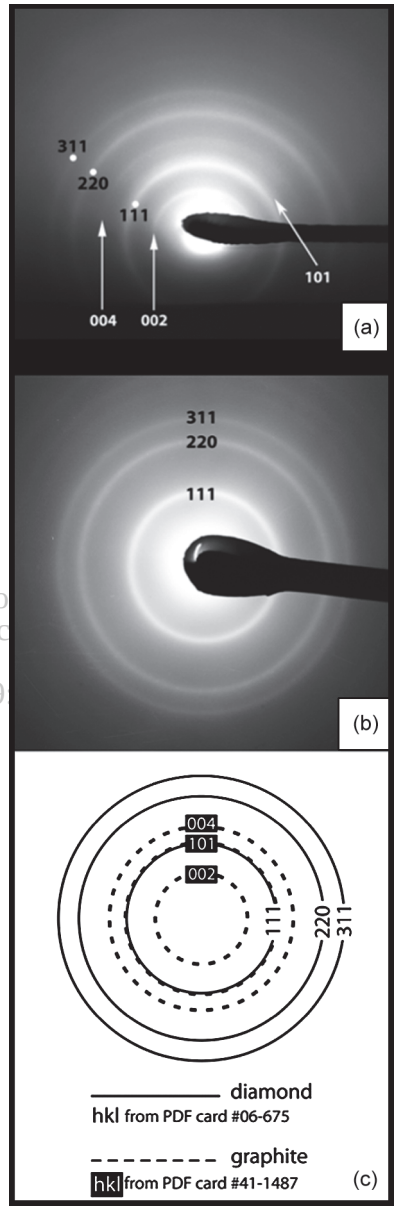

Fig. 3. ED patterns for sample A1 (a) and sample A2 (b) with the corresponding hkl indexing. In (a) the white dots and arrows put in evidence the diffraction rings due to the presence of diamond and graphite phase, respectively. The calculated ED pattern due to the simultaneous presence of diamond and graphite phases is reported in (c); For the simulation, the three highest diffraction intensities has been considered both for diamond and graphite, using the reference data from JCPDS PDF cards #06-675 and #41-1487, respectively.

1325 cm^{-1}, slightly red shifted with respect to that of bulk diamond (1332 cm^{-1}). For sample A1 (Fig. 4(a)), another spectral feature is the signal at about 1600 cm^{-1}, that, according to,[18] can be ascribed to G-bands of nanographite sp^2 carbon species.

For sample A2, the spectral features at about 1500 cm^{-1}, together with that one at about 1350 cm^{-1}, is indicative of the presence of large amounts of amorphous carbon species. Moreover, for sample A2 the peak at 1150 cm^{-1}

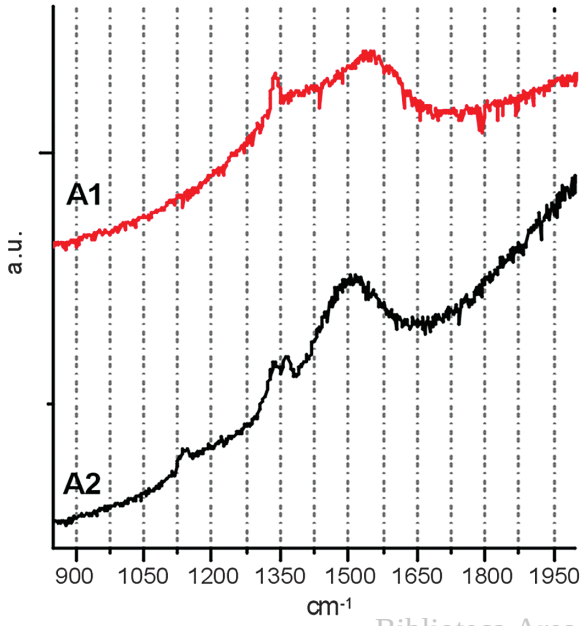

Fig. 4. Raman spectra of samples A1 and A2.

and the shoulder at about 1450 cm^{-1} indicate the presence of the transpolyacetylene specie.[19]

The appearance of a luminescence background in both the sample could be related to diamond fluorescence, but it can be also due to hydrogenated amorphous carbon.[20]

Overall, the Raman spectrum of sample A1 is consistent with the presence of nanodiamond crystallites with some nanographite contamination; instead the Raman spectrum of sample A2 looks like the spectra of ultrananodiamond deposits[21] with the presence of amorphous *C* and trans-polyacetylene species.

Even if it has proved difficult to track experimentally the dynamic of the building process able to generate the diamond nanocones during a single-step deposition run, the growth of these structures may be ascribed to a competition between the rates of concomitant reactions. The growing up of the diamond phase starts from the condensation on the substrate surface of sp^3-coordinated carbon atoms and their clustering into seeds that evolve producing isolated diamond nanograins. Under our experimental conditions, the building up of the diamond entities by progressive addition of C clusters is balanced by the process of etching due to the energetic H ions impinging at right angle on the negatively polarized substrate. The etching process acts preferentially on the top of the growing structures, where fast removal of the diamond materials is found to occur and further addictions of C-sp^3 clusters from the gas phase are prevented. The balance between the growing rate and the etching rate across the height of the protruding diamond structures could thus explain their final conical features. The two geometrical shapes can be then rationalized considering a different ratio between growing and etching rate: in the case of sample A2, due to the larger amount of C source, this ratio could be larger and may justify the ascending helicoidal ramps that grow around a cone, as evidenced in Figure 2.

Given such notable features and the spatial arrangement, our tipped nanodiamond deposits appear to be promising structures to be used in systems for electron emission.

Before the FE measurements, in order to stabilize the emission current, we carried out a conditioning step by applying a moderate electric field, according to the procedure detailed in Ref. [24]. For sample A1 the conditioning process has been rather fast. For sample A1 three or four V sweeps were sufficient to eliminate adsorbates and obtain a stable and reproducible emission, whereas for sample A2 the emitted current *versus* time was found rough even after long conditioning process.

Figure 5 shows the trend of the emitted current versus the electric field for sample A1 (Fig. 5(a)) and A2 (Fig. 5(b)). Some subsequent runs of measurement are reported for the two samples. In the in-sets are reported the corresponding Fowler-Nordheim (FN) curves. Sample A1 is definitively characterized by higher emission properties that will be discussed in the following.

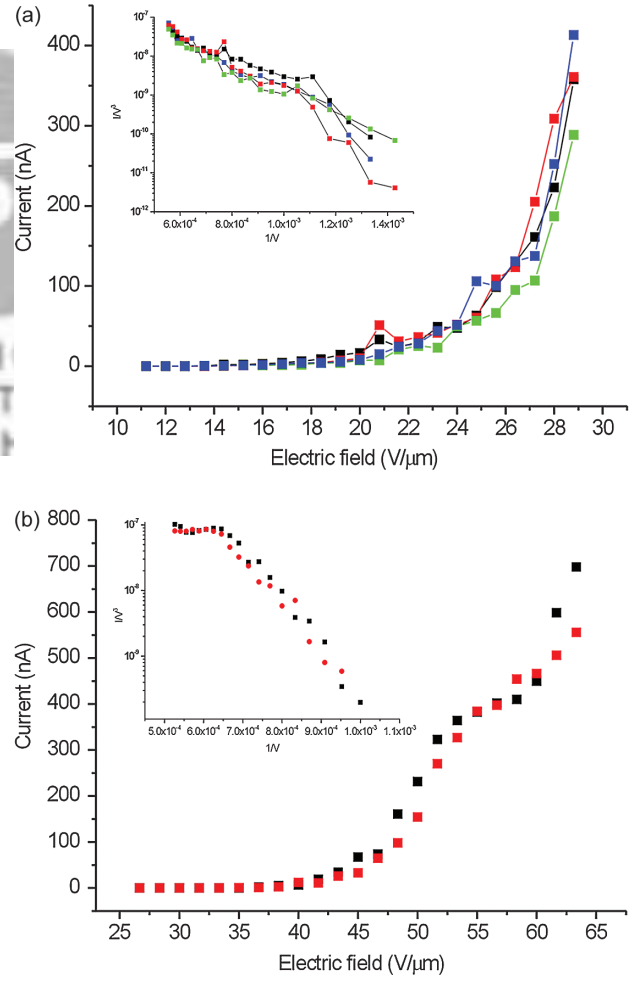

Fig. 5. Emitted current versus the electric field for sample A1 (a) and A2 (b). In the in-set are reported the corresponding FN curves.

The FE characteristics have been extracted from I/V data using the analytical method described in Ref. [22]. The turn-on field (corresponding to an electron emission of 1 nA) was found to be 15 V/μm and the maximum density current at 1800 V (28 V/μm) 1.3 mA/cm^2. For the β factor a value of 10 has been evaluated. A good stability of the emission was demonstrated during prolonged working cycles. The reproducibility and stability of the emission are accompanied by a lack of discharges or spikes even during long-lasting measurements.

These characteristics are better than that reported for whiskers obtain by means of O_2 plasma etching,[3] but worse than those for ordered arrays of sub-micron diamond tips.[4]

Refs. [3] and [4] refer to polycrystalline diamond samples constituted by sub-micron or micrometric crystallites of high crystalline quality without significant graphite or amorphous *C* contamination.

The emission from ultra nanodiamond on carbon nanofibers[23] exhibits a behaviour similar to that of our nanocones. It is to be noted however that the best FE properties are exhibited by nanodiamond grown on carbon nanotubes.[24]

The analysis and comparison of the above reported results deserve some comments. Field emission from diamond can be described as a three steps process: injection, transport, and emission. The diamond is characterized by a negative electron affinity (NEA). Moreover in diamond nanocones (but also whiskers and pillars) the field concentration (beta factor) due to the high aspect ratio can strongly improve emission current. All these factors: diamond structure and NEA, conductive or injection channel have to be taken into account in the discussion of FE data from nanodiamond structures, along with the shielding effect related to the array density.

The negative electron affinity of diamond provides ideal sites for electron emission without any barriers. Therefore, the transport of electrons from bulk to surface is a key factor in order to sustain a stable and high current emission. In such a context, grain boundaries and graphite patches provides a great number of transport channels for electrons (as well as alternative emission sites).

The emission from sample A1 exhibits a better behaviour than the one from A2 in term of threshold, current density and stability and this finding is consistent with a structure consisting of a prevalent nanosized diamond phase mixed to a small amount of C-sp^2 in form of nano graphite (acting as conductive channel).

The low value of the beta factor could likely be related to the high surface density of cones and to the consequent shielding of electric field that affects the current density values.

For sample A2 both Raman and RHEED analysis seem to indicate a structure similar to that of an amorphous sp^3/sp^2 C material and this is reflected in FE properties. Moreover the instability of the emitted current can be explained considering that the carbon polymeric species (i.e., transpolyacetylene) are unstable and can easily be desorbed during electron emission.

4. CONCLUSIONS

We are developing a CVD methodology based on the use a MW-RF dual-mode reactor to produce arrays of nanostructured diamond cones by a single-step process. The emission behaviour of a series of diamond nanocones samples produced under different experimental conditions has been thoroughly investigated. The reported analysis is focussed on two types of nanocone deposits, characterised by rather different shapes: tipped and helicoidal cones. The FE measurements from these samples evidenced that the differences in emission properties are strictly connected to the crystalline features of diamond at the nanoscale and to the presence of a C-sp^2 phase. In particular, for the examined samples, the emission threshold, the current density and the emission stability showed marked differences, that could be rationalized taking into account the main factors affecting the emission mechanisms. In addition to the structural features, one must indeed consider also field concentration, NEA, shielding effects and presence of injection channels.

In case of cones consisting of nanodiamond crystallites with a relatively low nanographitic contaminations and requiring a very fast conditioning, a maximum current density of 1.3 mA/cm^2, and stable emission were detected. The rather good emission properties well relate to the specific structure of the sample, with a favourable enhancement factor given by the shape of the elongated structures, and make this material useful for the realization of technological promising cold cathodes. Even if the currents emitted from the conical nanodiamond deposits here presented are not as high as those found for other diamond-based samples, it must be underlined that the present structures have been produced by a one-step CVD process.

The proposed bottom-up methodology enables the scaling-up for deposition on larger areas as well as a facile integration in microelectronic devices, overcoming the design restrictions and high costs associated with conventional RIE treatments made on diamond films.

Acknowledgments: This work has been partially supported by the Italian MIUR through the PRIN2008 project: "*Advanced nanomaterials and nanostructures for field- and photo-emission based devices*."

References and Notes

1. T. Tyler, V. V. Zhirnov, A. V. Kvit, D. Kang, and J. J. Hren, *Appl. Phys. Lett.* 82, 2906 (**2003**).
2. Y. Andoa, Y. Nishibayashi, H. Furuta, K. Kobashi, T. Hirao, and K. Oura, *Diamond Relat. Mater.* 12, 168i (**2003**).

3. C. Y. Li and A. Hatta, *Diamond Relat. Mater.* 14, 1780 (**2005**).
4. E. S. Baik, Y. J. Baik, and D. Jeon, *Thin Solid Films* 377, 299 (**2000**).
5. M. D. Stoikou, P. John, and J. I. B. Wilson, *Diamond Relat. Mater.* 17, 1164 (**2008**).
6. W. Janssen and E. Gheeraert, *Diamond Relat. Mater.* 20, 389 (**2011**).
7. W. J. Zhang, Y. Wu, C. Y. Chan, W. K. Wong, X. M. Meng, I. Bello, Y. Lifshitz, and S. T. Lee, *Diamond Relat. Mater.* 13, 1037 (**2004**).
8. Y. Ando, Y. Nishibayashi, and A. Sawabe, *Diamond Relat. Mater.* 13, 633 (**2004**).
9. L. T. Sun, J. L. Gong, Z. Y. Zhu, D. Z. Zhu, and S. X. He, *Adv. Mater.* 16, 1849 (**2004**).
10. A. R. Sobia, G. J. Yu, and X. T. Zhou, *J. Cryst. Growth* 13, 33328 (**2009**).
11. R. Arenal, P. Bruno, D. J. Miller, M. Bleuel, J. Lai, and D. M. Gruen, *Phys. Rev. B* 75, 195431 (**2007**).
12. S. A. Rakha, G. Yu, J. Cao, S. He, and X. Zhou, *Diamond Relat. Mater.* 19, 284 (**2010**).
13. M. L. Terranova, S. Orlanducci, A. Fiori, E. Tamburri, V. Sessa, M. Rossi, and A. S. Barnard, *Chem. Mat.* 17, 3214 (**2005**).
14. M. L. Terranova, S. Orlanducci, E. Tamburri, V. Guglielmotti, F. Toschi, D. Hampai, and M. Rossi, *Nanotechnology* 19, 415601 (**2008**).
15. M. L. Terranova, V. Guglielmotti, S. Orlanducci, V. Sessa, D. Sordi, E. Tamburri, F. Toschi, L. Palumbo, A. Valloni, and M. Rossi, *Crystallography Reports* 55, 1223 (**2010**).
16. S. Orlanducci, F. Toschi, V. Guglielmotti, E. Tamburri, M. L. Terranova, and M. Rossi, *Nanoscience and Nanotechnology Letters* 3, 83 (**2011**).
17. F. Toschi, S. Orlanducci, V. Guglielmotti, I. Cianchetta, C. Magni, M. L. Terranova, M. Pasquali, E. Tamburri, R. Matassa, and M. Rossi, *Chem. Phys. Lett.* (**2012**), accepted.
18. M. A. Pimenta, G. Dresselhaus, M. S. Dresselhaus, L. G. Cancado, A. Jorio, and R. Saito, *Phys. Chem. Chem. Phys.* 9, 1276 (**2007**).
19. A. C. Ferrari and J. Robertson, *Phys. Rev. B* 63, 121405R (**2001**).
20. M. A. Tamor and W. C. Vassel, *J. Appl. Phys.* 76, 3823 (**1994**).
21. T. Ikeda, K. Teii, C. Casiraghi, J. Robertson, and A. C. Ferrari, *J. Appl. Phys.* 104, 073720 (**2008**).
22. I. Boscolo, S. Cialdi, A. Fiori, M. L. Terranova, A. Ciorba, M. Rossi, and M. J. Vac, *Science and Techn. B* 25, 1253 (**2007**).
23. X. Xiao, O. Auciello, H. Cui, D. H. Lowndes, V. L. Merkulov, and J. Carlisle, *Dia. Rel. Mat.* 15, 244 (**2006**).
24. S. Orlanducci, A. Fiori, V. Sessa, E. Tamburri, F. Toschi, and M. L. Terranova, *J. Nanosci. Nanotechnol.* 8, 3228 (**2008**).

Received: 26 August 2011. Accepted: 16 November 2011.